Strathprints Institutional Repository

http://strathprints.strath.ac.uk/

Europium doping of zincblende GaN by ion implantation

K. Lorenz,[1,2,a)] I. S. Roqan,[3] N. Franco,[1,2] K. P. O'Donnell,[3] V. Darakchieva,[1,2] E. Alves,[1,2] C. Trager-Cowan,[3] R. W. Martin,[3] D. J. As,[4] and M. Panfilova[4]

[1]*Instituto Tecnológico e Nuclear, EN10, 2686-953 Sacavem, Portugal*
[2]*CFNUL, Av. Prof. Gama Pinto 2, 1649-003 Lisboa, Portugal*
[3]*Department of Physics, SUPA, University of Strathclyde, Glasgow G4 0NG, United Kingdom*
[4]*Department of Physics, University of Paderborn, 33098 Paderborn, Germany*

Eu was implanted into high quality cubic (zincblende) GaN (ZB-GaN) layers grown by molecular beam epitaxy. Detailed structural characterization before and after implantation was performed by x-ray diffraction (XRD) and Rutherford backscattering/channeling spectrometry. A low concentration ($<10\%$) of wurtzite phase inclusions was observed by XRD analysis in as-grown samples with their (0001) planes aligned with the {111} planes of the cubic lattice. Implantation of Eu causes an expansion of the lattice parameter in the implanted region similar to that observed for the c-lattice parameter of wurtzite GaN (W-GaN). For ZB-GaN:Eu, a large fraction of Eu ions is found on a high symmetry interstitial site aligned with the $\langle 110 \rangle$ direction, while a Ga substitutional site is observed for W-GaN:Eu. The implantation damage in ZB-GaN:Eu could partly be removed by thermal annealing, but an *increase* in the wurtzite phase fraction was observed at the same time. Cathodoluminescence, photoluminescence (PL), and PL excitation spectroscopy revealed several emission lines which can be attributed to distinct Eu-related optical centers in ZB-GaN and W-GaN inclusions. © *2009 American Institute of Physics*. [DOI: 10.1063/1.3138806]

I. INTRODUCTION

Group III nitrides are promising host materials for optically active rare earth (RE) ions due to their wide and direct bandgaps which allow energetic RE^{3+} levels of the $4f$-shell emitting in the visible and ultraviolet wavelengths regions.[1] Prototypes of electroluminescent devices emitting in the whole visible region were reported for GaN doped with RE ions during growth by molecular beam epitaxy (MBE).[2] Eu-doped wurtzite GaN (W-GaN) has been widely studied due to its intense red light emission near ~ 621 nm in epitaxial films doped *in situ* or by ion implantation and in GaN powders.[1–14] In implanted and MBE *in situ* doped W-GaN films, the RE ions are incorporated preferentially into substitutional or slightly displaced Ga sites.[5,15,16] Nevertheless, depending on the sample preparation, several Eu-related optically active centers were observed.[10,13,14] Interestingly, only one of the two main centers observed in *in situ* doped samples showed stimulated emission.[13] Furthermore, implanted and MBE *in situ* doped samples show very similar luminescence spectra.[14] However, the exact excitation mechanisms and the microscopic nature of different centers are still under debate.[1]

Besides the wurtzite structure, GaN can also crystallize in the metastable cubic (zincblende) structure (ZB-GaN). ZB-GaN, typically grown on cubic GaAs or $3C$-SiC substrates, shows attractive properties such as the possibility of cleaving and the absence of spontaneous electric polarization which reduces the efficiency of optoelectronic devices based on wurtzite nitrides.[17–19] However, the crystal quality of currently available ZB-GaN is still lower than state-of-the-art

W-GaN; in particular, it suffers from the incorporation of wurtzite phase inclusions.[19] Very few reports exist on RE doping of ZB-GaN and on ion implantation in this material.[20–23] Kozanecki *et al.*[20] reported a single luminescence center for Er-implanted ZB-GaN and proposed that Er is incorporated on an interstitial site. Roqan *et al.*[21] described the emissions of Eu-implanted ZB-GaN where the results were influenced by the partial conversion of ZB-GaN to W-GaN after implantation and annealing. Also some authors discussed the magnetic properties of Mn- and Gd-implanted ZB-GaN but no detailed structural investigation of ion implanted ZB-GaN is reported.[22,23]

In this work, we study the structural and optical properties of Eu-implanted ZB-GaN grown by MBE and show that implantation damage can be partly removed by thermal annealing. However, x-ray diffraction (XRD) shows that the volume fraction of wurtzite phase inclusions is increased by the thermal treatment. Cathodoluminescence (CL), photoluminescence (PL), and PL excitation (PLE) measurements reveal various Eu-related red emission lines with different excitation behaviors which we assign to Eu ions incorporated into ZB-GaN and W-GaN inclusions. Lattice site location measurements using the Rutherford backscattering/channeling (RBS/C) technique show that, unlike the case of W-GaN, Eu is *not* incorporated on substitutional Ga sites but a large fraction is found on a high symmetry site aligned with the $\langle 110 \rangle$ direction.

II. EXPERIMENTAL DETAILS

ZB-GaN samples with a thickness of ~ 700 nm were grown at 720 °C by MBE on cubic $3C$-SiC (001) substrates. Details of sample growth were published in Ref. 24. Strong

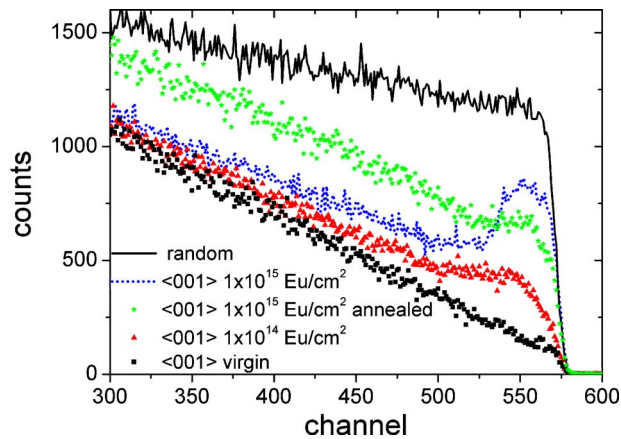---

a)Electronic mail: lorenz@itn.pt.

FIG. 1. (Color online) A typical random and ⟨001⟩ aligned RBS/C spectra after Eu implantation at 300 keV into ZB-GaN to different fluences. For the higher fluence the spectrum after annealing at 1000 °C is also presented. The aligned spectrum of a virgin sample is shown for comparison.

band edge PL at 379.3 nm for laser excitation above the bandgap evidences the high quality of the layers. Implantation of Eu ions was performed to fluences of 1×10^{14} and 1×10^{15} at./cm^2 with 300 or 150 keV at room temperature (RT) along the ⟨001⟩ direction. The Eu profile was measured by RBS and showed the maximum Eu concentration of ~0.2 at. % at a depth of ~42 nm for the sample implanted with the higher fluence. Postimplantation annealing was performed for 20 min at temperatures between 800 and 1000 °C in a tubular furnace under 1 bar N$_2$ pressure using a W-GaN proximity cap.

RBS/C measurements were performed to assess crystalline quality, implantation damage, and the lattice site location of Eu using 2 MeV He$^+$ ions and silicon surface barrier detectors at scattering angles of 160° and close to 180°. Detailed angular scans were performed with a two-axis goniometer with an accuracy of 0.01°.

XRD reciprocal space maps (RSMs) were acquired using monochromatic Cu $K\alpha_1$ radiation on a high resolution diffractometer equipped with a Göbel mirror, a two-bounce Ge(444) monochromator and a position-sensitive detector. XRD rocking curves and pole figures were measured on a D8Discover system from Bruker-AXS using an asymmetric two-bounce Ge(220) monochromator and a scintillation detector.

Low temperature CL was studied by using a home-built CL spectrometer. High resolution (0.05 nm) CL spectra (at 20 K) were obtained with an electron beam of 5 keV energy and $3-5$ μA current. PL (at 15 K) was excited using a He–Cd laser (325 nm). Selective PLE was carried out on samples at 20 K, using the output of a xenon (Xe) lamp (~1000 W) filtered by a $\frac{1}{4}$ m monochromator. All the PLE spectra were corrected for the wavelength variation of the lamp/monochromator output.

III. RESULTS AND DISCUSSION

A typical random and ⟨001⟩ aligned RBS/C spectra for an as-grown (virgin) ZB-GaN sample and samples implanted to fluences of 1×10^{14} and 1×10^{15} at./cm^2 are presented in Fig. 1. Close to the surface the virgin sample shows mini-

mum yields (yield in the aligned spectrum divided by the random yield) of 10%, 16%, and 19% for the ⟨110⟩, ⟨001⟩, and ⟨111⟩ directions, respectively. The lowest value of the minimum yield observed for the ⟨110⟩ axis is expected since in the zincblende structure this is the best channeling direction characterized by large and open channels. The dechanneling rate is high and the backscattering yield increases linearly with depth throughout the entire GaN layer. Minimum yields are considerably higher than for W-GaN which shows a typical value of 2% along the [0001] axis. However, it should be noted that even in W-GaN the channeling quality along tilted directions is much lower than for the [0001] growth direction probably because dislocations are mainly of edge type oriented parallel to the *c*-axis and due to mosaicity showing twists around the [0001] direction. This is the case for the ⟨10$\bar{1}$1⟩ axis where the minimum yield is higher and a stronger dechanneling is evidenced by a linear increase in the backscattering yield with depth similar to that seen in ZB-GaN (see, for example, Ref. 25). The high minimum yield and dechanneling rate are caused by native defects and wurtzite phase inclusions [stacking faults (SFs)]; the constant dechanneling rate indicates that these defects are distributed homogeneously in the ZB-GaN film. The presence and orientation of these inclusions were confirmed and studied by measuring XRD pole figures of the ZB-GaN {224} and the W-GaN {101} planes. For this the open detector was fixed at the expected 2θ value for these reflections and full azimuthal Φ-scans were acquired for tilt angles Ψ between 0° and 70°. It was shown that the (0001) planes of W-GaN inclusions are parallel to the {111} planes of ZB-GaN. The W-GaN inclusions are mainly aligned with only two of the four equivalent ⟨111⟩ directions in ZB-GaN, rotated by 90° with respect to each other.

After implantation the backscattering from the implanted region increases due to the implantation damage. It is interesting to compare the damage profiles in ZB-GaN with those observed for W-GaN under identical implantation conditions:[26] while implanted W-GaN typically shows two damage regions, one at the surface and one in the bulk close to the end of range of the implanted ions, implanted ZB-GaN exhibits only one damage peak, in the bulk. Like W-GaN, ZB-GaN shows strong resistance to implantation damage; for the higher fluence of 1×10^{15} at./cm^2, the damage stays well below the random level, showing that no amorphization takes place for the moderate fluences studied here.

Figure 2 presents the RSMs around the 002 reciprocal lattice point of ZB-GaN: as-grown [Fig. 2(a)], after implantation of 1×10^{14} at./cm^2 [Fig. 2(b)], and after annealing of the implanted sample at 900 °C [Fig. 2(c)]. After Eu implantation the RSM shows an elongation of the peak from ZB-GaN toward the lower values of the reciprocal space coordinate Q_z indicating an increase in the out-of-plane lattice parameter in the implanted region [Fig. 2(b)]. The average lattice dilation along the [001] direction in the implanted region of this sample is about 0.7%. This expansion is reversed by thermal annealing due to the annihilation of lattice defects rather than the incorporation of Eu into the lattice sites [Fig. 2(c)]. An expansion of the *c*-lattice parameter after
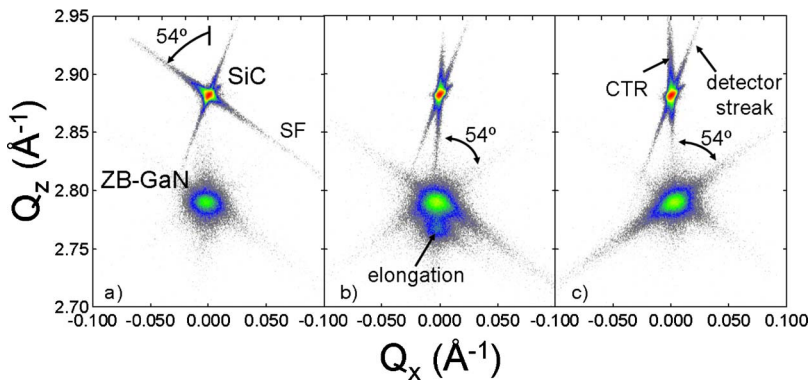
FIG. 2. (Color online) XRD RSM around the 002 reciprocal lattice point of ZB-GaN: (a) virgin sample, (b) after implantation of 1×10^{14} at./cm^2 Eu ions at 300 keV, (c) implanted sample after annealing at 900 °C. In (c) the streaks corresponding to the CTR and to the detector are marked.

implantation is also common in W-GaN.[27] The common streaks present in all maps are due to the saturation of the position sensitive detector and in some of them the crystal truncation rod (CTR) is visible [see Fig. 2(c)]. The streak across the SiC reflex marked SF [see Fig. 2(a)] has an angle of ~54° toward the surface normal which can be associated with SFs in the {111} planes of SiC.[28] The remaining starlike streaks of scattered intensity across the ZB-GaN 002 reflex also form an angle of ~54° with the surface normal which corresponds to the angle between the {111} planes and the crystal surface. These streaks may be associated with SF lying in the {111} planes of ZB-GaN which give rise to the wurtzite phase inclusions.

Figure 3 shows the angular RBS/C scans for Eu and Ga across the ⟨001⟩ and ⟨110⟩ axes after an implantation of 1×10^{15} at./cm^2 Eu ions at 300 keV. The measurements indicate that Eu is distributed randomly within the ⟨001⟩ channel (the yield for Eu scatters around 1) but it is aligned with the atomic rows along the ⟨110⟩ direction (the scan for Eu clearly shows a dip with the same width as the Ga scan). These results are in good agreement with Ref. 20 on optical spectroscopic investigations of Er-implanted ZB-GaN which indicate that Er is incorporated in regular interstitial sites. In contrast to this, in W-GaN the REs are preferentially found on, or near, substitutional Ga sites.[16]

Annealing at 1000 °C partly removes the implantation damage, as seen by the more pronounced minimum of the Ga dip (Fig. 3), particularly along the ⟨110⟩ direction. The Eu scans do not change significantly after annealing (not shown) indicating that the fraction of Eu occupying the regular interstitial site is not affected by the annealing. The random and aligned RBS/C spectra before and after annealing (Fig. 1) show the decrease in direct backscattering at defects in the implanted region. However, the backscattering from the deeper regions of the ZB-GaN layer increases indicating a deterioration of the crystal also in the unimplanted bulk region due to the annealing.

In fact, detailed studies using XRD rocking curves of the 002 reflection of ZB-GaN and the 101 reflection of W-GaN inclusions show that the volume fraction of W-GaN material increases during annealing. The fraction of wurtzite material was estimated by summing up the integrated intensity of the 101 rocking curves for the four different orientations [parallel to the {111} planes of ZB-GaN]. The ratio with the integrated intensity of the 002 reflection of ZB-GaN can be directly used to estimate the W-GaN volume fraction since the

theoretically predicted intensity from the {002} planes in ZB-GaN is very similar to that of {101} planes in W-GaN.[29] According to this estimate the W-GaN fraction increased from less than 10% in the virgin samples to nearly 50% after annealing at 900 °C. Similar results are found in unimplanted but annealed samples showing that the implantation itself plays a minor role in the process of phase conversion. The extent of phase conversion does depend strongly on the phase purity of the as-grown material. Note that the annealing temperature lies well above the growth temperature of the ZB-GaN which promotes the conversion of the metastable zincblende phase to the stable wurtzite phase.

The good crystal quality of the virgin layers in this study is demonstrated by a strong ZB-GaN near band edge (NBE) emission at 379.3 nm upon optical excitation at 325 nm (Fig. 4); very weak yellow emission has also been observed. The phase conversion evidenced by XRD also influences the PL spectra; after annealing the emission intensity at 379.3 nm decreases and a new peak becomes visible at 355 nm corresponding to the NBE emission of W-GaN. Furthermore, it is interesting to note that the line at ~394.5 nm, generally assigned to donor-acceptor pair transitions,[30] increases after annealing which points to a connection of this line with the hexagonal phase inclusions or SFs. PLE measurements (Fig. 5) of as-grown ZB-GaN showed a well defined absorption edge with a maximum at ~375 nm when monitoring at a wavelength of 450 nm which corresponds to a broad and
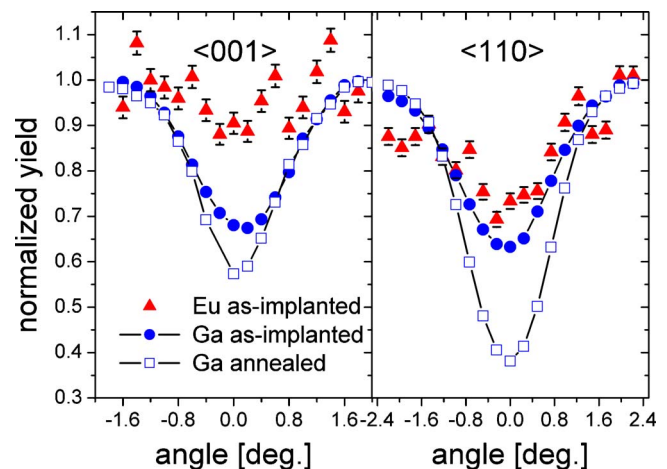

FIG. 3. (Color online) RBS/C channeling scans (before and after annealing at 1000 °C) across the ⟨001⟩ and ⟨110⟩ axes of ZB-GaN implanted with 1×10^{15} at./cm^2 Eu ions at 300 keV.
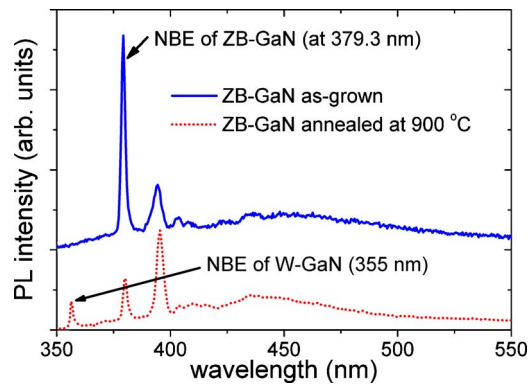
FIG. 4. (Color online) PL spectra of an as-grown and an unimplanted but annealed ZB-GaN sample taken at 15 K with excitation at 325 nm. The upper spectrum was shifted for clarity.

FIG. 6. (Color online) Low temperature CL spectra of Eu-implanted (150 keV, 1×10^{15} Eu/cm^2) W-GaN (annealed at 1000 °C) and ZB-GaN (annealed at 900 and 800 °C).

weak (probably defect-related) luminescence band (see Fig. 4). Figure 6 presents low temperature CL spectra for ZB-GaN implanted with 1×10^{15} at./cm^2 at 150 keV Eu after annealing at 800 and 900 °C. A spectrum of a Eu-implanted W-GaN layer is also shown. Similar to our previous results in samples with lower quality,[21] the three main lines found in W-GaN:Eu at 620.7, 621.7, and 622.5 nm are also present in the ZB-GaN:Eu samples due to Eu incorporated in W-GaN inclusions. Additional lines at 623.5 and 627 nm and several peaks at higher wavelength are visible in the sample annealed at 800 °C and are assigned to Eu incorporated at a number of sites in the cubic lattice. Their relative intensity decreases with the annealing temperature as the conversion of ZB-GaN to W-GaN progresses, as shown in Fig. 6. In contrast to previous results,[21] the 623.5 nm line is seen in the CL spectra up to RT. The line at 627 nm becomes the dominant line in the PL spectra for excitation below the bandgap of ZB-GaN:Eu.[21] The assignment of the emission lines to Eu in ZB-GaN or W-GaN is further confirmed by PLE measurements performed on the lines at 627 and 621 nm (Fig. 5). The line at 621 nm is efficiently excited only at energies above the W-GaN band edge at 355 nm in agreement with the assumption that this line arises from Eu centers in W-GaN.[10] When the intensity is monitored at 627 nm, two absorption bands are observed, one strong band below the

bandgap of ZB-GaN (which could represent, according to accepted excitation models, an "Eu-associated defect" or "charge-transfer state" localized in the bandgap) and a weaker one coinciding with the bandgap at ~380 nm (this excitation was absent for preliminary measurements of Ref. 21 probably due to optical "masking" of the cubic material by the predominant wurtzite phase), while the excitation efficiency drops for higher energy excitation. The pronounced drop of excitation between 390 and 370 nm might be related to a low energy transfer cross section to the Eu^{3+} ions for band-to-band excitation. The fact that Eu was not found on substitutional lattice sites might play a role in this context. Another explanation would be that the Eu centers emitting at 627 nm are too deep inside the sample and a strong absorption of ZB-GaN inhibits their excitation with light above the bandgap. This explanation, however, seems unlikely because the composition and structural quality of the samples are homogeneous with depth and the implantation only reaches an ~100 nm thick surface layer. The prominent line at 623.5 nm as well as the lines above 630 nm observed in the CL spectrum of the sample annealed at 800 °C and assigned to ZB-GaN:Eu are not visible in PL spectra irrespective of the excitation wavelength which points to the presence of multiple Eu centers in ZB-GaN:Eu with different excitation properties.

IV. CONCLUSIONS

Eu was implanted into high quality ZB-GaN grown by MBE on 3C-SiC substrates. The implantation damage causes an expansion of the out-of-plane lattice parameter, similar to that observed for the c-lattice parameter in W-GaN. Unlike the case of W-GaN no preferential surface damage was observed for implantation in ZB-GaN which is promising because this highly damaged layer causes a degradation of the surface during postimplantation annealing. However, partial conversion of ZB-GaN to W-GaN was observed during annealing above the ZB-GaN growth temperature. A large fraction of Eu was found on a high symmetry interstitial site in contrast to W-GaN:Eu where Eu is nearly substitutional on Ga sites. Optical activation was achieved after annealing and
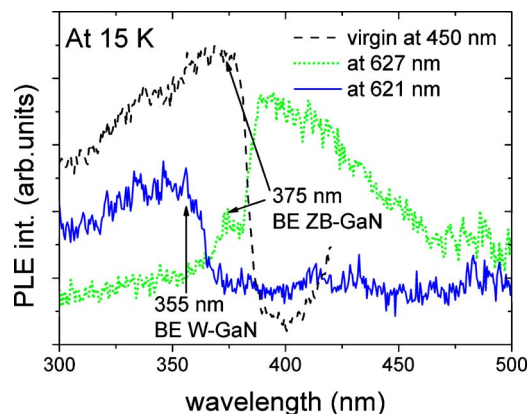

FIG. 5. (Color online) PLE spectra of ZB-GaN monitored at 450 nm in the virgin sample and on the Eu lines at 627 and 621 nm after implantation of 1×10^{15} Eu/cm^2 at 300 keV and annealing at 1000 °C.
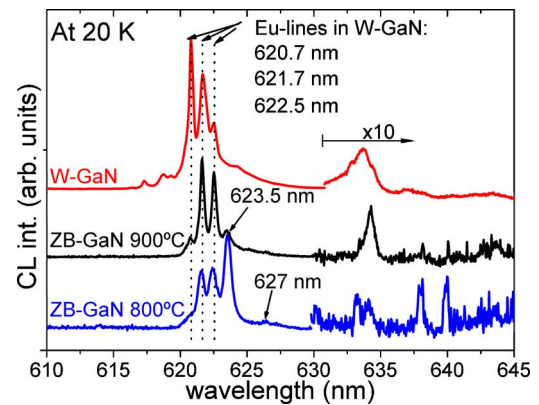
different Eu emission lines could be assigned to Eu centers in cubic ZB-GaN and Eu centers residing within W-GaN inclusions.

ACKNOWLEDGMENTS

[1]K. P. O'Donnell and B. Hourahine, Eur. Phys. J.: Appl. Phys. **36**, 91 (2006).
[2]A. J. Steckl, J. C. Heikenfeld, D. S. Lee, M. J. Garter, C. C. Baker, Y. Wang, and R. Jones, IEEE J. Sel. Top. Quantum Electron. **8**, 749 (2002).
[3]J. C. Heikenfeld, M. Garter, D. S. Lee, R. Birkhahn, and A. J. Steckl, Appl. Phys. Lett. **75**, 1189 (1999).
[4]H. J. Lozykowski, W. M. Jadwisienczak, J. Han, and I. G. Brown, Appl. Phys. Lett. **77**, 767 (2000).
[5]T. Monteiro, C. Boemare, M. J. Soares, R. A. Sá Ferreira, L. D. Carlos, K. Lorenz, R. Vianden, and E. Alves, Physica B **308**, 22 (2001).
[6]O. Contreras, S. Srinivasan, F. A. Ponce, G. A. Hirata, F. Ramos, and J. McKittrick, Appl. Phys. Lett. **81**, 1993 (2002).
[7]E. E. Nyein, U. Hömmerich, J. Heikenfeld, D. S. Lee, A. J. Steckl, and J. M. Zavada, Appl. Phys. Lett. **82**, 1655 (2003).
[8]K. Lorenz, U. Wahl, E. Alves, S. Dalmasso, R. W. Martin, K. P. O'Donnell, S. Ruffenach, and O. Briot, Appl. Phys. Lett. **85**, 2712 (2004).
[9]Y. Hori, X. Biquard, E. Monroy, D. Jalabert, F. Enjalbert, L. S. Dang, M. Tanaka, O. Oda, and B. Daudin, Appl. Phys. Lett. **84**, 206 (2004).
[10]K. Wang, R. W. Martin, K. P. O'Donnell, V. Katchkanov, E. Nogales, K. Lorenz, E. Alves, S. Ruffenach, and O. Briot, Appl. Phys. Lett. **87**, 112107 (2005).
[11]R. Kudrawiec, M. Nyk, A. Podhorodecki, J. Misiewicz, W. Strek, and M. Wołcyrz, Appl. Phys. Lett. **88**, 061916 (2006).
[12]H. Wu, C. B. Poitras, M. Lipson, M. G. Spencer, J. Hunting, and F. J. DiSalvo, Appl. Phys. Lett. **88**, 011921 (2006).
[13]J. H. Park and A. J. Steckl, Appl. Phys. Lett. **88**, 011111 (2006).
[14]L. Bodiou, A. Braud, J.-L. Doualan, R. Moncorgé, J. H. Park, C. Munasinghe, A. J. Steckl, K. Lorenz, E. Alves, and B. Daudin, J. Appl. Phys. **105**, 043104 (2009).
[15]K. Lorenz, R. Vianden, R. Birkhahn, A. J. Steckl, M. F. da Silva, J. C. Soares, and E. Alves, Nucl. Instrum. Methods Phys. Res. B **161–163**, 946 (2000).
[16]U. Wahl, E. Alves, K. Lorenz, J. G. Correia, T. Monteiro, B. De Vries, A. Vantomme, and R. Vianden, Mater. Sci. Eng., B **105**, 132 (2003).
[17]D. Schikora, M. Hankeln, D. J. As, K. Lischka, T. Litz, A. Waag, T. Buhrow, and F. Henneberger, Phys. Rev. B **54**, R8381 (1996).
[18]H. Okumura, K. Ohta, G. Feuillet, K. Balakrishnan, S. Chichibu, H. Hamaguchi, P. Hacke, and S. Yoshida, J. Cryst. Growth **178**, 113 (1997).
[19]B. Daudin, G. Feuillet, J. Hübner, Y. Samson, F. Widmann, A. Philippe, C. Bru-Chevallier, G. Guillot, E. Bustarret, G. Bentoumi, and A. Deneuville, J. Appl. Phys. **84**, 2295 (1998).
[20]A. Kozanecki, V. Glukhanyuk, and H. Przybylinska, Phys. Status Solidi A **205**, 38 (2008).
[21]I. S. Roqan, K. P. O'Donnell, C. Trager-Cowan, B. Hourahine, R. W. Martin, K. Lorenz, E. Alves, D. J. As, M. Panfilova, and I. M. Watson, Phys. Status Solidi B **245**, 170 (2008).
[22]V. A. Chitta, J. A. H. Coaquira, J. R. L. Fernandez, C. A. Duarte, J. R. Leite, D. Schikora, D. J. As, K. Lischka, and E. Abramof, Appl. Phys. Lett. **85**, 3777 (2004).
[23]F. Y. Lo, A. Melinkov, D. Reuter, A. D. Wieck, V. Ney, T. Kammermeier, A. Ney, J. Schörmann, S. Potthast, D. J. As, and K. Lischka, Appl. Phys. Lett. **90**, 262505 (2007).
[24]J. Schörmann, S. Potthast, D. J. As, and K. Lischka, Appl. Phys. Lett. **90**, 041918 (2007).
[25]J. G. Marques, K. Lorenz, N. Franco, and E. Alves, Nucl. Instrum. Methods Phys. Res. B **249**, 358 (2006).
[26]K. Lorenz, U. Wahl, E. Alves, E. Nogales, S. Dalmasso, R. W. Martin, K. P. O'Donnell, M. Wojdak, A. Braud, T. Monteiro, T. Wojtowicz, P. Ruterana, S. Ruffenach, and O. Briot, Opt. Mater. (Amsterdam, Neth.), **28**, 750 (2006).
[27]B. Pipeleers, S. M. Hogg, and A. Vantomme, J. Appl. Phys. **98**, 123504 (2005).
[28]A. Boulle, D. Chaussende, L. Latu-Romain, F. Conchon, O. Masson, and R. Guinebretière, Appl. Phys. Lett. **89**, 091902 (2006).
[29]H. Tsuchiya, K. Sunaba, and S. Yonemura, Jpn. J. Appl. Phys., Part 2 **36**, L1 (1997).
[30]D. J. As, F. Schmilgus, C. Wang, B. Schöttker, D. Schikora, and K. Lischka, Appl. Phys. Lett. **70**, 1311 (1997).